PHILOSOPHICAL TRANSACTIONS OF THE ROYAL SOCIETY A MATHEMATICAL, PHYSICAL & ENGINEERING SCIENCES

X-Ray Emission Analysis in the Electron Microscope

D. A. Jefferson

Phil. Trans. R. Soc. Lond. A 1982 **305**, 535-543
doi: 10.1098/rsta.1982.0050

Phil. Trans. R. Soc. Lond. A **305**, 535–543 (1982)
Printed in Great Britain

X-ray emission analysis in the electron microscope

By D. A. Jefferson
Department of Physical Chemistry, Lensfield Road, Cambridge CB2 1EP, U.K.

[Plates 1–3]

The technique by which sample-emitted X-rays are recorded in the electron microscope is assessed. Although the method is relatively insensitive for elements of low atomic number, its applicability in the field of *simultaneous* structural and compositional investigations is discussed, together with a critical examination of the analytical precision possible. Various examples of its use are described, including some where structure and stoichiometry can be determined in crystals containing fewer than 10^{10} atoms.

1. Introduction

Before the last decade, analytical and solid-state structural chemistry have essentially developed separately. These two fields of chemistry have always been related, largely from the requirement that, unless the composition of material under study is accurately known, full structural analysis is generally impossible. Nevertheless, there has been no experimental connection between the two aspects of investigation. This has certainly applied to standard methods of structure determination, where material of predetermined composition is subjected to X-ray or neutron diffraction analysis, and also in more modern spectroscopic methods such as infrared, Mössbauer and nuclear magnetic resonance techniques. In all investigations of this type, where quantities of material studied are of the order of 10^{-2} g or more, good analytical data are a necessary prelude to structure solution, which then takes place separately.

The methods of structure determination listed above have one aspect in common, this being that they produce information that represents an average over the whole specimen, normally containing some 10^{22} atoms. Indeed the very essence of a diffraction experiment is to obtain the average Fourier transform of an object. Structural homogeneity is not a prerequisite of diffraction studies, but if specimens are inhomogeneous little indication of this is revealed, and an average result is still obtained. Consequently, an independently determined average composition is normally quite adequate for correlating with the structural information derived.

In recent years, however, solid-state chemists, particularly those concerned in the inorganic field, have turned their attention to systems where the degree of structural or compositional inhomogeneity or both is very great. Furthermore, it is frequently this very inhomogeneity that is the chief object of study. Such systems are frequently the products of solid-state reactions, which may well be incomplete, or more subtle assemblages such as the infinitely adaptive phases described by Anderson (1973). In these cases, separate structural and compositional studies are of little value, and a requirement exists for the production of simultaneous structural and compositional data. Consequently the two aspects of study can no longer be considered separately, and a technique combining both has to be employed. So far, the most successful has beeen electron microscopy in its various forms, which has the ability both to provide

structural data from either diffraction or imaging methods with specimens containing as few as 10^6–10^7 atoms, and to give chemical information from similar areas, involving the detection of elements in what may be high local but vanishingly small total concentration.

2. X-ray emission analysis

The various processes occurring when accelerated electrons interact with matter have been well documented. A recent review of these is given by Egerton (this symposium). Although the technique of electron energy-loss spectroscopy is generally regarded as the most powerful method for obtaining chemical information from electron–specimen interactions, largely

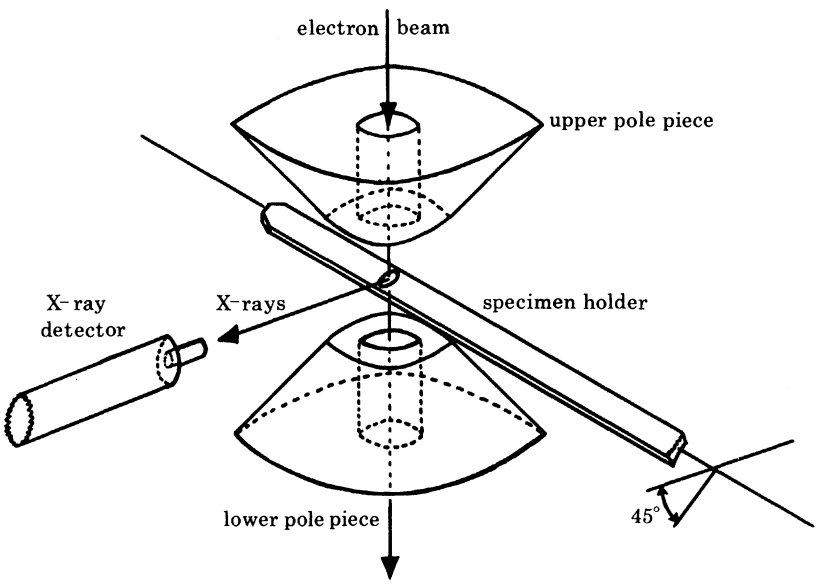

Figure 1. Schematic arrangement of the specimen area in a typical analytical electron microscope. For clarity, anti-contamination devices and aperture holders are omitted.

because of its applicability to all elements and its intrinsically high spatial resolution, the recording of the X-ray emission spectrum from the specimen irradiated by the electron beam is far more extensively used. This mainly arises from the less stringent requirements on specimen dimensions, particularly thickness, in the latter method, and indeed, for combined structural and compositional analysis of elements heavier than sodium, X-ray emission spectroscopy has a virtual monopoly of the field, except where very high spatial resolution (*ca.* 3 nm) is required.

X-ray emission analysis is not a particularly new technique, being first employed in the electron probe microanalyser (e.p.m.a.) (Hillier 1947; Castaing & Guinier 1949). X-ray emission analysis in the electron microscope is basically a simple modification of the e.p.m.a. technique first described by Duncumb (1963). A typical modern experimental geometry is indicated in figure 1. In most conventional transmission microscopes, the specimen is in the form of a 3 mm diameter grid, which is enclosed in a specimen holder rod passing between the pole pieces of the objective lens. For structural investigation, facilities are available for tilting the specimen about mutually perpendicular axes such that appropriate electron diffraction patterns or images can be recorded. After this, the specimen holder is tilted such that the

X-rays generated at the specimen reach a suitable detector, usually of the lithium drifted silicon type, and the emission spectrum is recorded. Facilities also exist for scanning the electron beam in the form of an ultra-fine probe (of as little as 0.5 nm diameter in specialized scanning transmission instruments) across the specimen.

The analytical technique employed is inherently simple, but when used in a conventional electron microscope the arrangement must be a compromise between conditions optimized for analysis and those for the highest microscopic performance. The immediate benefit is that both structural and compositional information is available simultaneously. In addition, conventional microscopic samples are so thin that appreciable sideways scattering of electrons is slight, permitting smaller beam diameters at the specimen and consequently greater spatial resolution than in the e.p.m.a. However, in all other respects the e.p.m.a., optimized for analysis, is a superior instrument. In particular, the relatively high signal strength permits the detection of elements in concentrations as low as 100 $\mu g\ g^{-1}$ (Long 1977). The use of crystal spectrometer detectors permits a very high energy resolution, routinely of 1 eV, and allows the correlation of line shift with chemical environment (Fischer & Baun 1964; O'Nions & Smith 1971). Furthermore the use of a bulk specimen enables the volume irradiated to be calculated, permitting absolute concentrations of elements to be determined from the intensities of emission lines. By comparison, except in a very few favourable circumstances, only relative concentrations can be obtained from the emission spectrum of a typical microscope specimen.

3. Quantification

Given the shortcomings of the analytical electron microscope with respect to the e.p.m.a., it is necessary to assess the quality of the compositional information obtained. The detection limit is approximately 1 %, this being largely due to the high background. For purely qualitative work, emission spectra can be obtained in a variety of situations but, where quantitative analyses are required, special care is needed. A typical spectrum obtained is shown in figure 2. This was taken on a particle, subsequently identified as Cr_7S_8, in a mixture of chromium sulphides. It is clear that peaks due to sulphur Kα and Kβ and the corresponding lines of chromium can be readily identified, and also the copper Kα and Kβ lines arising from the specimen support. Although the instrumental resolution is insufficient to separate the two lines of sulphur, the peak areas of sulphur and chromium signals can be measured. Obtaining a quantitative analysis is then dependent on relating the ratio of these measurements to the elemental ratio in the specimen.

A comprehensive account of the corrections involved, in the context of e.p.m.a. operation, is given by Long (1977). Initially, allowance must be made for variation of detector sensitivity and inner-shell emission efficiency with energy. Both of these factors are calculable and present no problem. Allowance for processes occurring within the specimen itself (absorption of generated X-rays, X-ray fluorescence etc.) are grouped under the heading of matrix correction factors. In the bulk sample of the e.p.m.a. these are calculable by using iterative procedures (Sweatman & Long 1970), but no such treatment is possible in the thin samples used for transmission electron microscopy. Consequently, it has to be assumed (Cliff & Lorimer 1974) that the effect of these factors is negligible in thin specimens, an assumption that is generally justified in practical specimens, but which may break down in special cases. The final factor arising with analytical electron microscopes is that the specimen environment is not optimized

PHILOSOPHICAL TRANSACTIONS OF THE ROYAL SOCIETY A MATHEMATICAL, PHYSICAL & ENGINEERING SCIENCES

for analysis. In any conventional microscope, the specimen is surrounded by anticontamination devices, aperture holders and a variety of other accessories; stray electrons striking these (or electrons backscattered from the specimen) can generate a spurious X-ray signal, such as the Cu Kα peak in figure 2. Even more serious is the possibility that these X-rays can then generate further X-rays by fluorescence in *all* the crystals of the specimen, not just those irradiated by

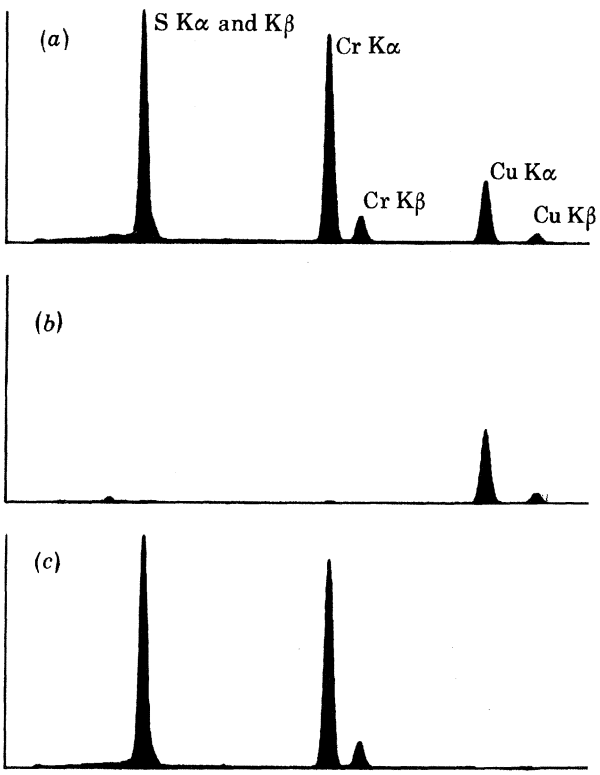

FIGURE 2. (*a*) X-ray emission spectra from a crystal of Cr_7S_8; (*b*) background spectrum; (*c*) subtracted spectrum.

the electron beam. This problem is particularly acute when samples containing Fe are supported by copper grids (Crawford 1980). Some estimate of these effects can be made by recording a background count with the electron beam impinging on a carbon support film. A background spectrum is also shown in figure 2, as is the result of subtracting this from the initial Cr_7S_8 spectrum. The procedure is not always completely reliable, however, and these latter factors are the most common sources of error in analyses made in the electron microscope.

4. APPLICATIONS

(*a*) *General analysis*

Applications of X-ray emission spectroscopy in the electron microscope are too numerous to be treated fully in a simple review. One of the most frequent tasks is the characterization of synthetic products. This is especially true in preparative inorganic chemistry, where characterization is generally a far more complex procedure than the actual synthesis. This results from the fact that the product may be extremely inhomogeneous, and if the phases present

PHILOSOPHICAL TRANSACTIONS OF THE ROYAL SOCIETY A MATHEMATICAL, PHYSICAL & ENGINEERING SCIENCES

have low symmetry their identification by means of bulk diffraction procedures is frequently impossible. Even without recourse to specific diffraction methods, such as electron diffraction, compositional differentiation can be difficult, if not impossible, in the e.p.m.a. owing to very small particle size. In such circumstances the analytical electron microscope can be of immense value, as a recent review of investigations of this type by Cheetham & Skarnoulis (1981) shows. Cases were illustrated where separate phases in mixed oxide and sulphide systems were correctly identified solely on the basis of chemical composition. New phases in the vanadium–molybdenum oxide system have also been identified in this way (A. K. Cheetham, unpublished data). This relatively simple and purely analytical method has also been applied successfully to biological fields (Hall 1974). All these examples are instances where the X-ray emission technique is used as the sole means of identification. More detailed studies, where both structural and compositional data are necessary, are given below in greater detail.

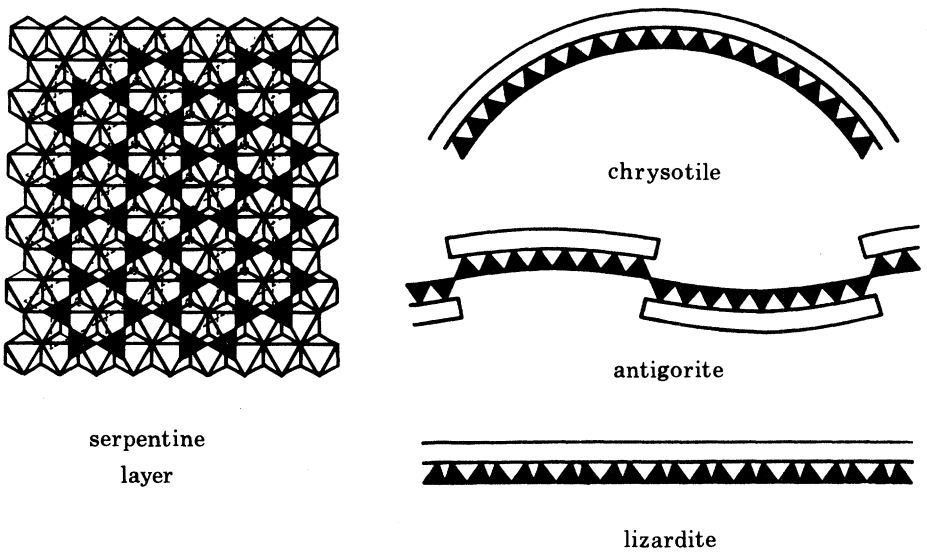

FIGURE 3. Schematic structural arrangement of the serpentine polymorphs. SiO_4 tetrahedra are shown as filled triangles.

(*b*) *Silicate systems*

Silicates are one of the prime examples of structural and compositional inhomogeneity, and X-ray emission analysis has proved extremely useful in identifying or confirming the existence of new phases or predicted intergrowths. An extremely topical instance is that given by Champness *et al.* (1976) in their evaluation of techniques necessary to identify the various forms of asbestos minerals. Employing a combination of medium resolution imaging, for morphological information, selected area electron diffraction and X-ray emission spectrometry, they concluded that the minerals chrysotile, crocidolite, amosite, anthophyllite, tremolite and actinolite could readily be identified, even when present only as atmospheric pollution, rather than in their normal mineral assemblages. Of these materials, chrysotile can generally be distinguished on the basis of morphological and electron diffraction evidence, but the others, being all double-chain silicates (amphiboles), present greater problems. However, they differ considerably in composition, and can thus be distinguished by X-ray emission spectroscopy, even when only present as single fibres.

One of the first instances of combined structural and co-positional studies made possible by X-ray emission analysis in the electron microscope was the examination of exsolution in orthopyroxenes by Champness & Lorimer (1973). Optical microscopy indicated that magnesium-rich orthopyroxenes exsolved a calcium-rich monoclinic pyroxene (augite) on cooling. In the sample studied by Champness & Lorimer, very fine lamellae of the augite phase were noted in medium resolution images, of width up to 0.5 μm. Selected area electron diffraction was used to confirm that lamellae were of monoclinic type, and X-ray emission analysis indicated, as expected, a high concentration of calcium in the exsolved phase. A more important discovery, however, lay in the observation of extremely fine plate-like precipitates between the augite lamellae. These could only be observed by direct imaging, and it was noted that they were absent in the matrix adjacent to the lamellae. The overall calcium concentration in this area was found to be extremely low. It was therefore concluded that these fine precipitates, which had been hitherto unsuspected, represented a 'kinetic compromise' structure that resulted from the slow diffusion of the calcium into the augite lamellae.

The ability to obtain structural data from images while obtaining compositional information from X-ray emission has been widely used in the study of microcrystalline silicates. Crawford (1980) has established a correlation between the stacking disorder–polytype formation and composition of complex layered silicates in this way, and Thomas *et al.* (1979) have investigated polymorphism in serpentines using similar methods. The different types of serpentine structure are shown in figure 3. Basically, they consist of a layer of edge-sharing $Mg(O,OH)_6$ octahedra bonded to a tetrahedral component incorporating corner-sharing SiO_4 groups. By using accepted ionic radii, it can easily be shown that a misfit exists between the two components, this being accommodated in the chrysotile form of serpentine by the layer curling up into a tube. An alternative form, where the layers are apparently flat but in reality corrugated, employs the same principles and is called antigorite. A third form, in which the layers are truly flat, lizardite, also exists, and is believed to result from the substitution of aluminium into both components, thus making the octahedral part smaller, and the tetrahedra larger, hence effectively removing the misfit. Unfortunately, this hypothesis has hitherto been difficult to test, bulk analytical techniques being of little use as the various forms usually occur together. However, examination of individual flakes (*ca.* 200–500 nm across) by combined high-resolution lattice imaging and X-ray emission analysis (figure 4, plate 1) readily confirms the presence of aluminium in lizardite flakes. Furthermore, the technique is sufficiently sensitive to detect slight aluminium concentrations in chrysotile tubes of abnormally large diameter, where the misfit between the two components, although not absent, is markedly reduced.

(*c*) *Oxide systems*

High resolution electron microscopic investigations of tungsten–niobium oxides were the first detailed studies of grossly non-stoichiometric materials on an ultrastructural scale (Allpress *et al.* 1972; Iijima & Allpress 1974). In such systems, the stoichiometry can essentially be elucidated directly from the image contrast. Recently, however, there has been an interest in other types of system where, even when the structure can be imaged with a point resolution exceeding 0.3 nm, the composition of the phases examined is by no means certain. One example of this type of study is in the field of bismuth tungstates. These structures, illustrated schematically in figure 5, are composed of Bi_2O_3 layers interleaved with varying numbers of WO_3 layers, constituting what is essentially a homologous series with stoichiometry $Bi_2W_nO_{3n+3}$.

PHILOSOPHICAL TRANSACTIONS OF THE ROYAL SOCIETY A MATHEMATICAL, PHYSICAL & ENGINEERING SCIENCES

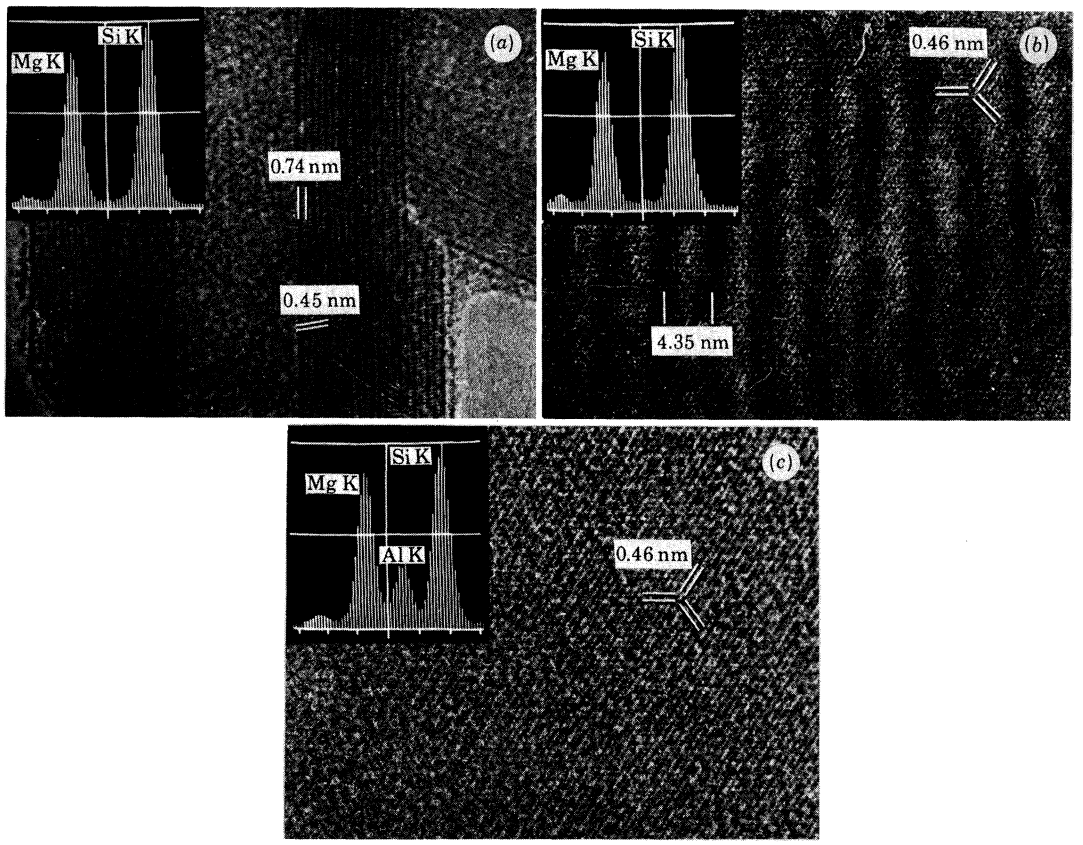

FIGURE 4. Combined high-resolution lattice images and X-ray emission spectra of (*a*) chrysotile, (*b*) antigorite and (*c*) lizardite.

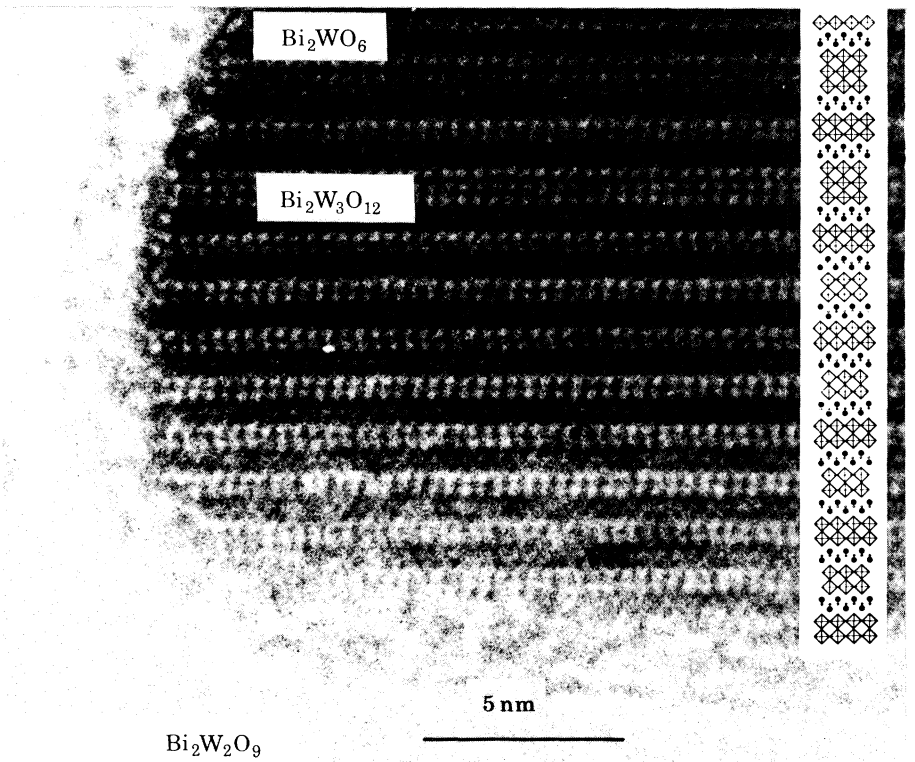

FIGURE 6. High-resolution lattice image of a crystal, predominantly $Bi_2W_2O_9$, showing intergrowths of $Bi_2W_3O_{12}$ and Bi_2WO_6. The electron beam was parallel to [110]. For comparison, a structure model is indicated.

(*Facing p.* 540)

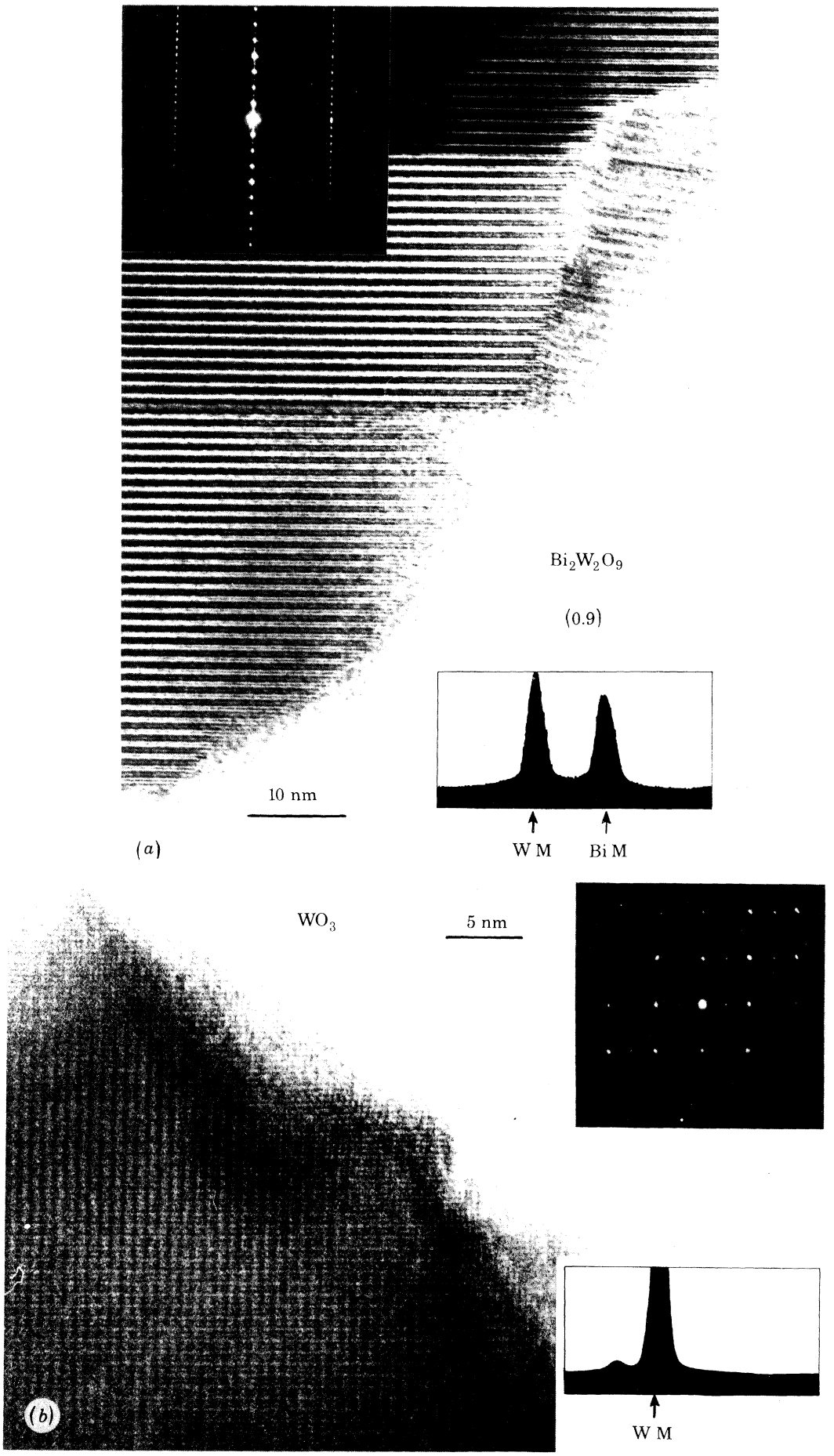

FIGURE 7. For description see opposite.

PHILOSOPHICAL TRANSACTIONS OF THE ROYAL SOCIETY A MATHEMATICAL, PHYSICAL & ENGINEERING SCIENCES

Description of plate 2

Figure 7. (*a*) Combined high-resolution lattice image, electron diffraction pattern and X-ray emission spectrum from a crystal of $Bi_2W_2O_9$. (*b*) As for (*a*), but with a crystal that proves to be pure WO_3.

PHILOSOPHICAL TRANSACTIONS OF THE ROYAL SOCIETY A MATHEMATICAL, PHYSICAL & ENGINEERING SCIENCES

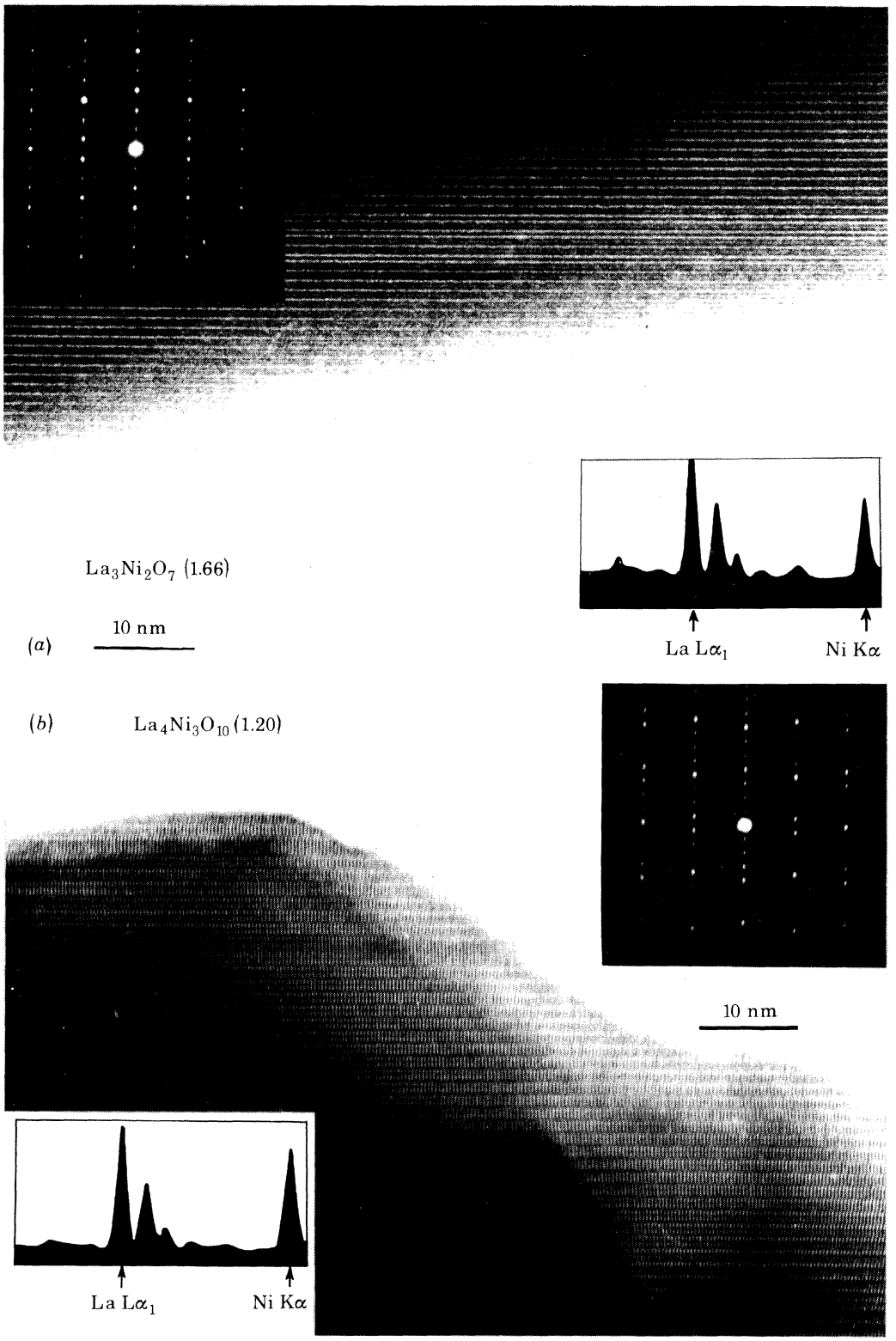

FIGURE 9. (*a*) Combined high-resolution lattice image, electron diffraction pattern and X-ray emission spectrum of a crystal of $La_3Ni_2O_7$. Defects in the structure are arrowed. (*b*) As for (*a*), but with a crystal of $La_4Ni_3O_{10}$.

PHILOSOPHICAL TRANSACTIONS OF THE ROYAL SOCIETY A MATHEMATICAL, PHYSICAL & ENGINEERING SCIENCES

The first two members of this series are known, but attempts to prepare the $n = 3$ member (Jefferson *et al.* 1982) by solid-state synthesis have not given well-crystalline products. The $Bi_2W_3O_{12}$ form has only been observed as unit-strip intergrowths in a matrix of $Bi_2W_2O_9$, as indicated in the high-resolution electron micrograph of figure 6, plate 1.

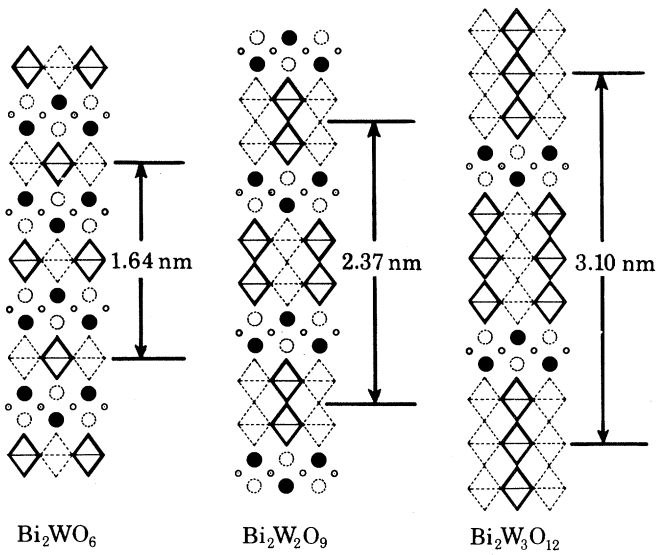

FIGURE 5. Schematic illustration of the first three members of the structural series $Bi_2W_nO_{3n+3}$, viewed along the [100] axis.

Unless the starting stoichiometry is wildly inaccurate, this then raises the question of where the extra WO_3 is accommodated. X-ray powder diffraction fails to indicate the presence of the free oxide, as the powder pattern is relatively complex. Two alternatives exist, namely that extra WO_3 could be accommodated within the apparently $Bi_2W_2O_9$ lattice, or that free WO_3 exists and is so finely crystalline that no evidence for it appears in the X-ray diffraction record. Simultaneous high-resolution imaging and X-ray emission analyses, as indicated in figure 7, plate 2, shows that the latter alternative is adopted. Crystals that are apparently $Bi_2W_2O_9$ do indeed have that composition, and some crystals of free WO_3 are found. It is of interest to note that, in the WO_3 crystal of figure 7*b*, the structure and diffraction pattern resemble that of $Bi_2W_2O_9$ in one projection, such that the two phases cannot be distinguished by diffraction evidence alone.

A similar example of elucidating a complex oxide system occurs in the lanthanum–nickel oxides. These consist essentially of intergrowths of the two phases $LaNiO_3$, a perovskite structure, and La_2NiO_4, a closely related phase. Intergrowths of varying numbers of the former with one unit of the latter can produce a homologous series of general stoichiometry $La_{n+1}Ni_nO_{3n+1}$ (figure 8). There are, however, several factors complicating this simple picture. In particular, electron diffraction studies (Drennan 1982) have shown that preparations with for example the composition $La_3Ni_2O_7$ exhibit severe stacking disorder. They also show a superlattice effect *within* the plane of the structural layers, suggesting that the structural picture is more complex than was first thought, and that the overall stoichiometry might not be that expected.

By using simultaneous high-resolution imaging and X-ray emission analysis, the structure–composition relation can be monitored directly. Figure 9, plate 3, shows some typical results

of an investigation of this type. The phase characterized by electron diffraction as $La_3Ni_2O_7$ (figure 9*a*) does have the intended composition, despite the presence of defects (arrowed) and a superlattice ordering, which is not visible in this particular projection. The material is polyphasic, however, and it is equally possible to find crystals of the type shown in figure 9*b*, which from diffraction evidence would correspond to the composition $La_4Ni_3O_{10}$. X-ray emission analysis of this crystal confirms this stoichiometry, and suggests that the La:Ni ratio

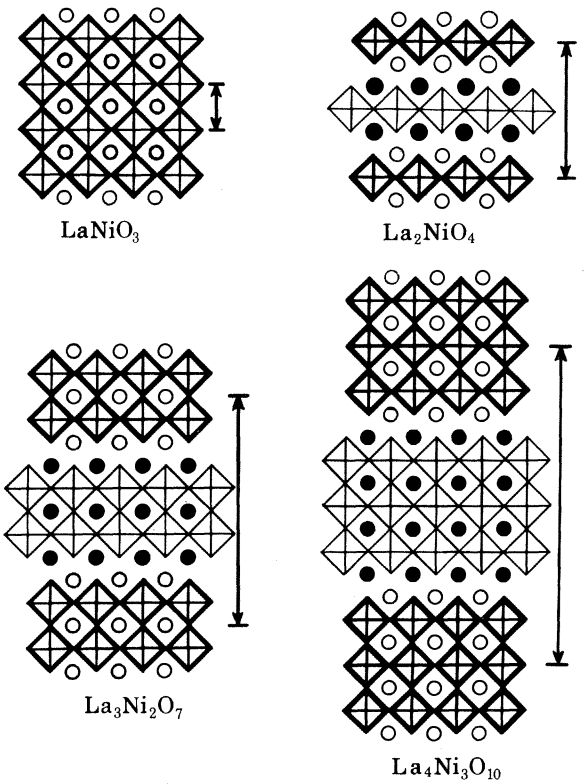

FIGURE 8. Schematic illustration of the first members of the structural series $La_{n+1}Ni_nO_{3n+1}$. La atoms are indicated by circles.

is in fact slightly less than 1.33, implying that the defects observed (arrowed) occur when extra strips of $LaNiO_3$, rather than $LaNiO_4$, are inserted into the structure. The relatively simple model for this structural series can therefore be confirmed directly, and the possibility of the so-called higher members being merely different stacking variants of the simpler structures can be entirely discounted.

5. Conclusions

The examples given above indicate the applicability of the X-ray emission analytical technique to electron microscopy. Although as purely analytical achievements their accuracy may be less than desired, their great importance is that they represent a new area of structural inorganic chemistry, namely the simultaneous determination of structure type and stoichiometry in crystals containing no more than 10^{10} atoms. Indeed, this figure can be reduced by several powers of ten if the so-called scanning transmission technique (Crewe 1974) is employed, at the expense of limiting structural data to electron diffraction only. With this degree of

spatial resolution, new areas of crystal chemistry, previously considered intractable, are now capable of solution.

I acknowledge the constant support of Professor J. M. Thomas, F.R.S., during the course of the original work described above. Thanks are also due to Professor B. C. H. Steele and Professor C. N. R. Rao for providing several of the samples used and for many useful discussions. Instrumentation was provided by the Science Research Council and this is gratefully acknowledged.

References (Jefferson)

Allpress, J. G., Hewart, E. A., Moodie, A. F. & Sanders, J. V. 1972 *Acta crystallogr.* A **28**, 528.
Anderson, J. S. 1973 *J. chem. Soc. Dalton Trans.*, p. 1107.
Castaing, R. & Guinier, R. 1949 In *Proceedings of the Conference on Electron Microscopy, Delft*, p. 60. The Hague: Martinus Nijhoff.
Champness, P. E. & Lorimer, G. W. 1973 *J. mater. Sci.* **8**, 467.
Champness, P. E., Cliff, G. & Lorimer, G. W. 1976 *J. Microsc.* **108**, 231.
Cheetham, A. K. & Skarnoulis, A. J. 1981 *Analyt. Chem.* **53**, 1060.
Cliff, G. & Lorimer, G. W. 1974 *J. Microsc.* **103**, 203.
Crawford, E. S. 1980 Ph.D. thesis, University of Wales.
Crewe, A. V. 1974 *J. Microsc.* **100**, 247.
Drennan, J. 1982 (In preparation.)
Duncumb, P. 1963 In *X-ray optics and X-ray microanalysis* (ed. H. H. Patece, V. E. Cosslett & A. Engstron), p. 431. New York: Academic Press.
Fischer, D. W. & Baun, W. L. 1964 *Adv. X-ray Anal.* **7**, 489.
Jefferson, D. A., Gopalakrishnan, P. & Ramanan, A. 1982 *Mater. Res. Bull.* **17**, 269.
Hall, T. A. 1974 *J. Microsc., Paris* **22**, 271.
Hillier, J. 1947 U.S. Patent no. 2,418,029.
Iijima, S. & Allpress, J. G. 1974 *Acta crystallogr.* A**30**, 29.
Long, J. V. P. 1977 In *Physical methods in determinative mineralogy* (ed. J. Zussman), p. 273. London: Academic Press.
O'Nions, R. K. & Smith, D. G. W. 1971 *Am. Miner.* **56**, 1452.
Sweatman, T. R. & Long, J. V. P. 1970 *J. Petr.* **10**, 332.
Thomas, J. M., Jefferson, D. A., Mallinson, L. G., Smith, D. J. & Crawford, E. S. 1979 *Chemica Scr.* **14**, 167.

PHILOSOPHICAL TRANSACTIONS OF THE ROYAL SOCIETY A MATHEMATICAL, PHYSICAL & ENGINEERING SCIENCES

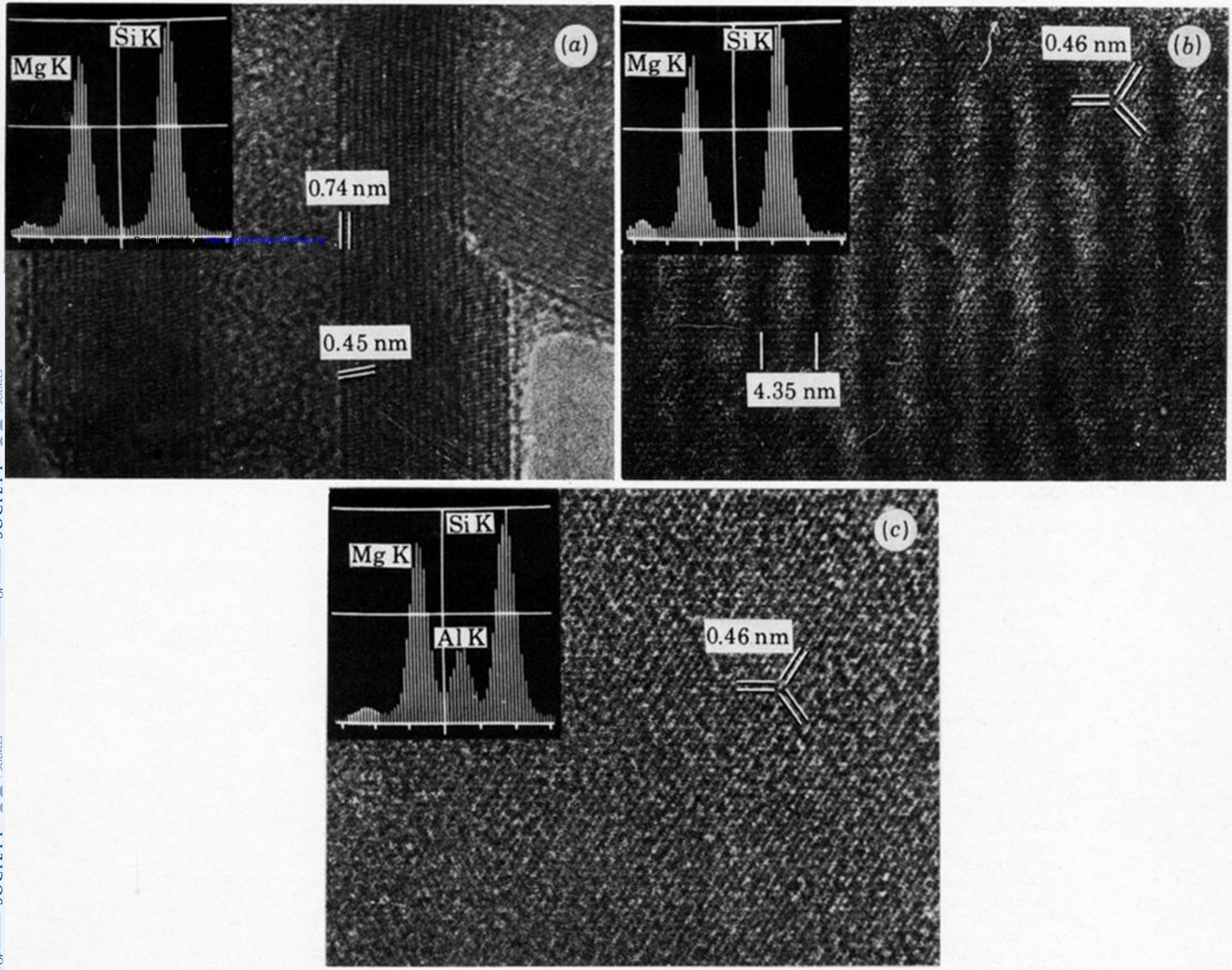

FIGURE 4. Combined high-resolution lattice images and X-ray emission spectra of (*a*) chrysotile, (*b*) antigorite and (*c*) lizardite.

PHILOSOPHICAL TRANSACTIONS OF THE ROYAL SOCIETY A MATHEMATICAL, PHYSICAL & ENGINEERING SCIENCES

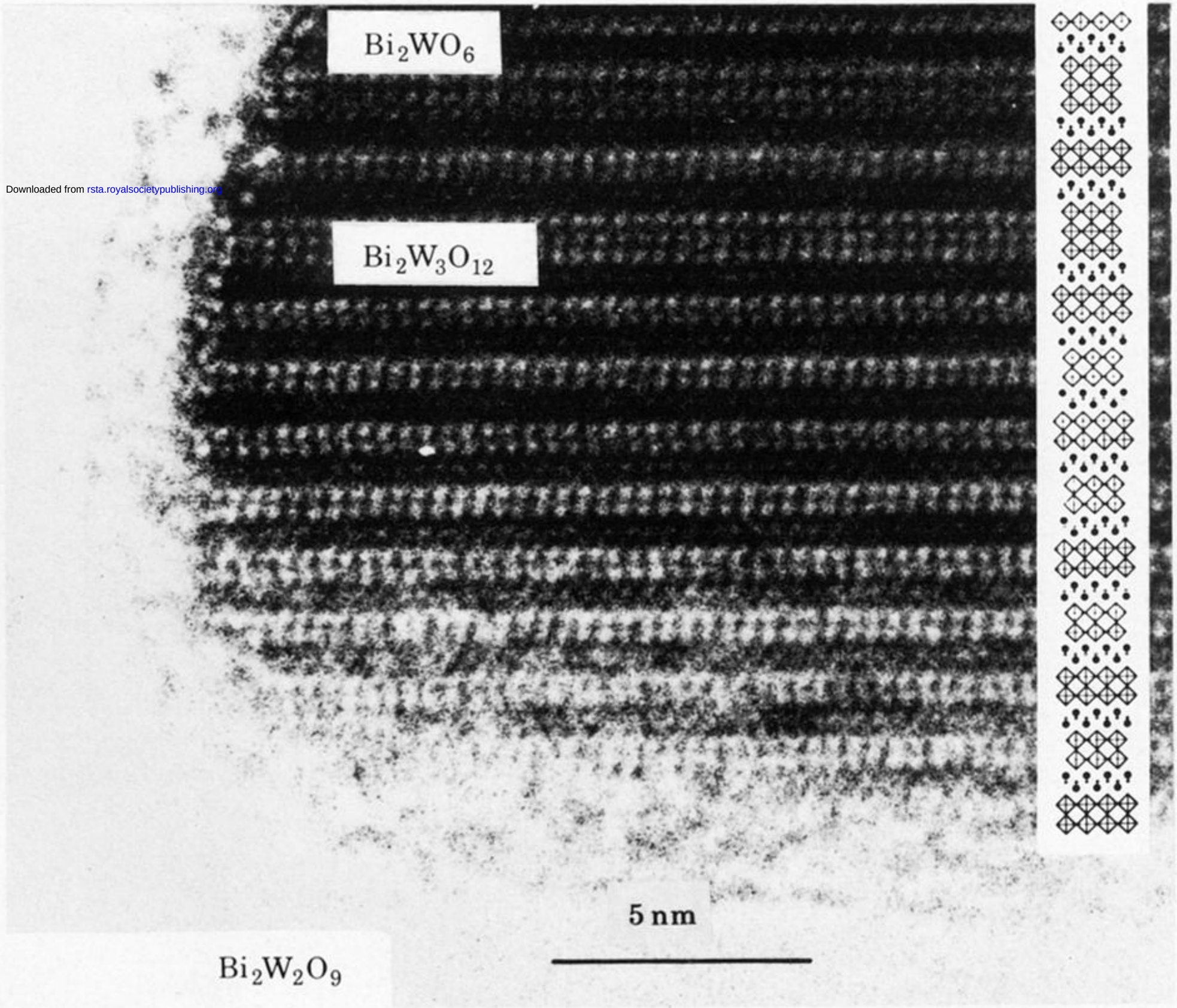

FIGURE 6. High-resolution lattice image of a crystal, predominantly $Bi_2W_2O_9$, showing intergrowths of $Bi_2W_3O_{12}$ and Bi_2WO_6. The electron beam was parallel to [110]. For comparison, a structure model is indicated.

PHILOSOPHICAL TRANSACTIONS OF THE ROYAL SOCIETY A MATHEMATICAL, PHYSICAL & ENGINEERING SCIENCES

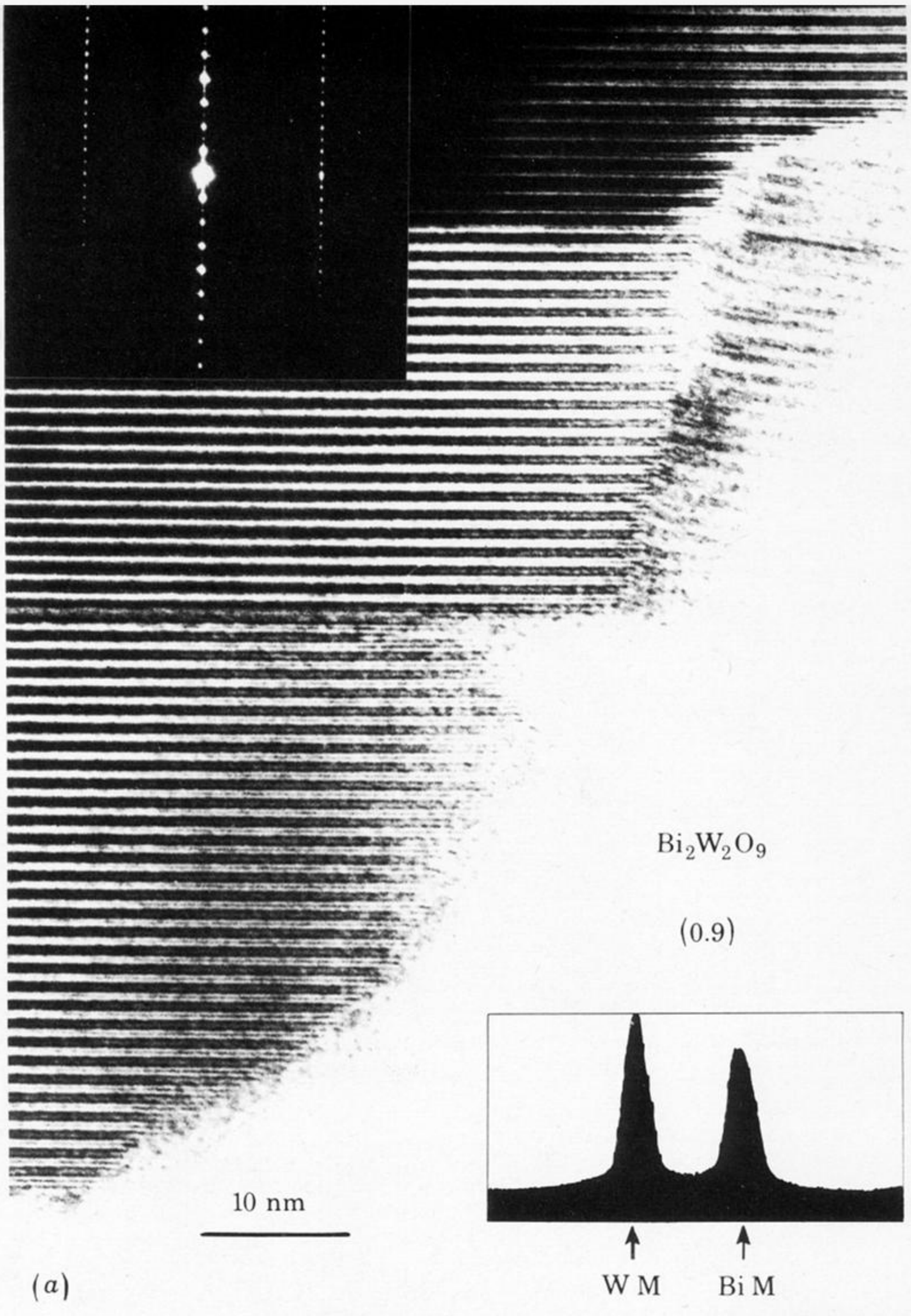

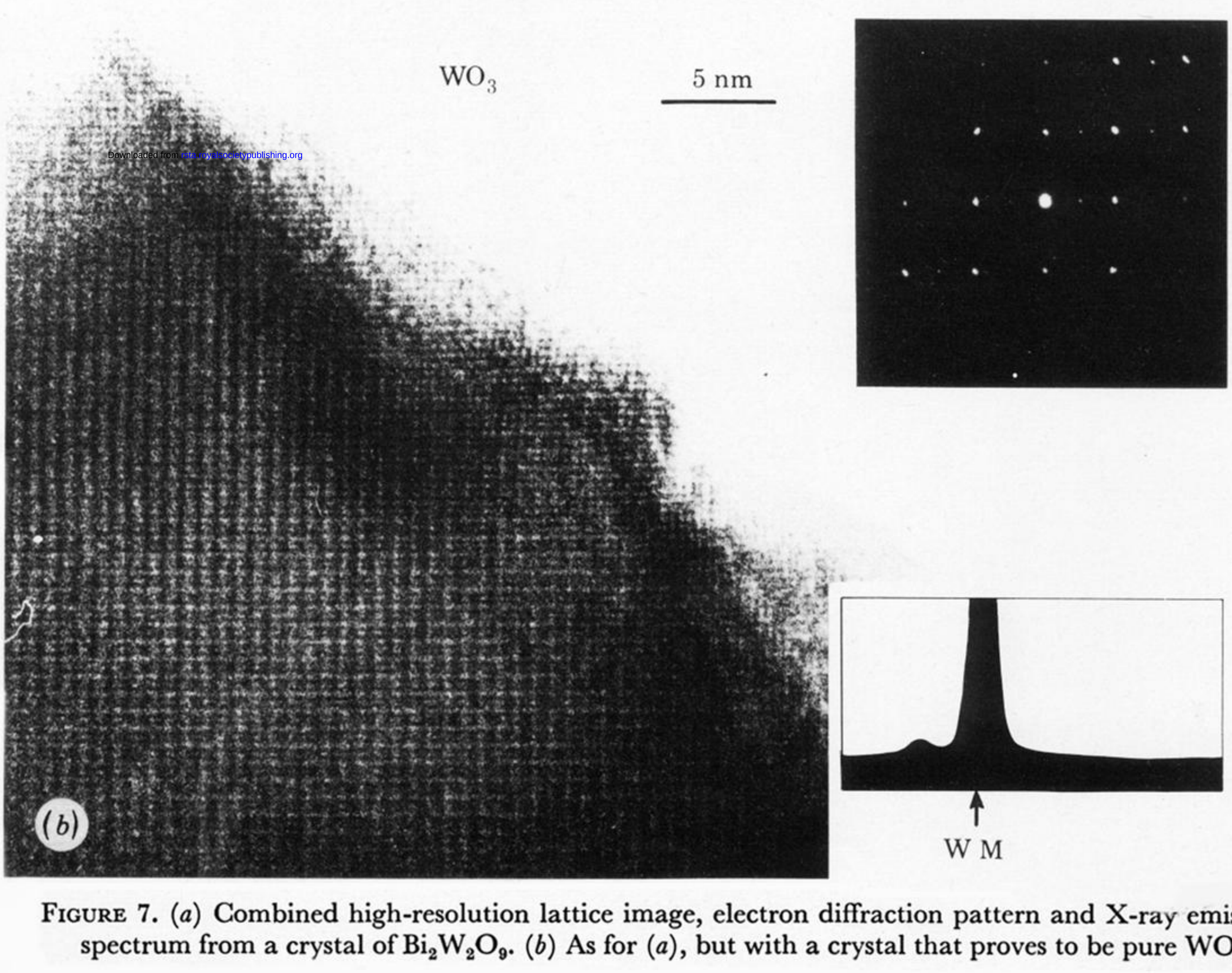

FIGURE 7. (*a*) Combined high-resolution lattice image, electron diffraction pattern and X-ray emission spectrum from a crystal of $Bi_2W_2O_9$. (*b*) As for (*a*), but with a crystal that proves to be pure WO_3.

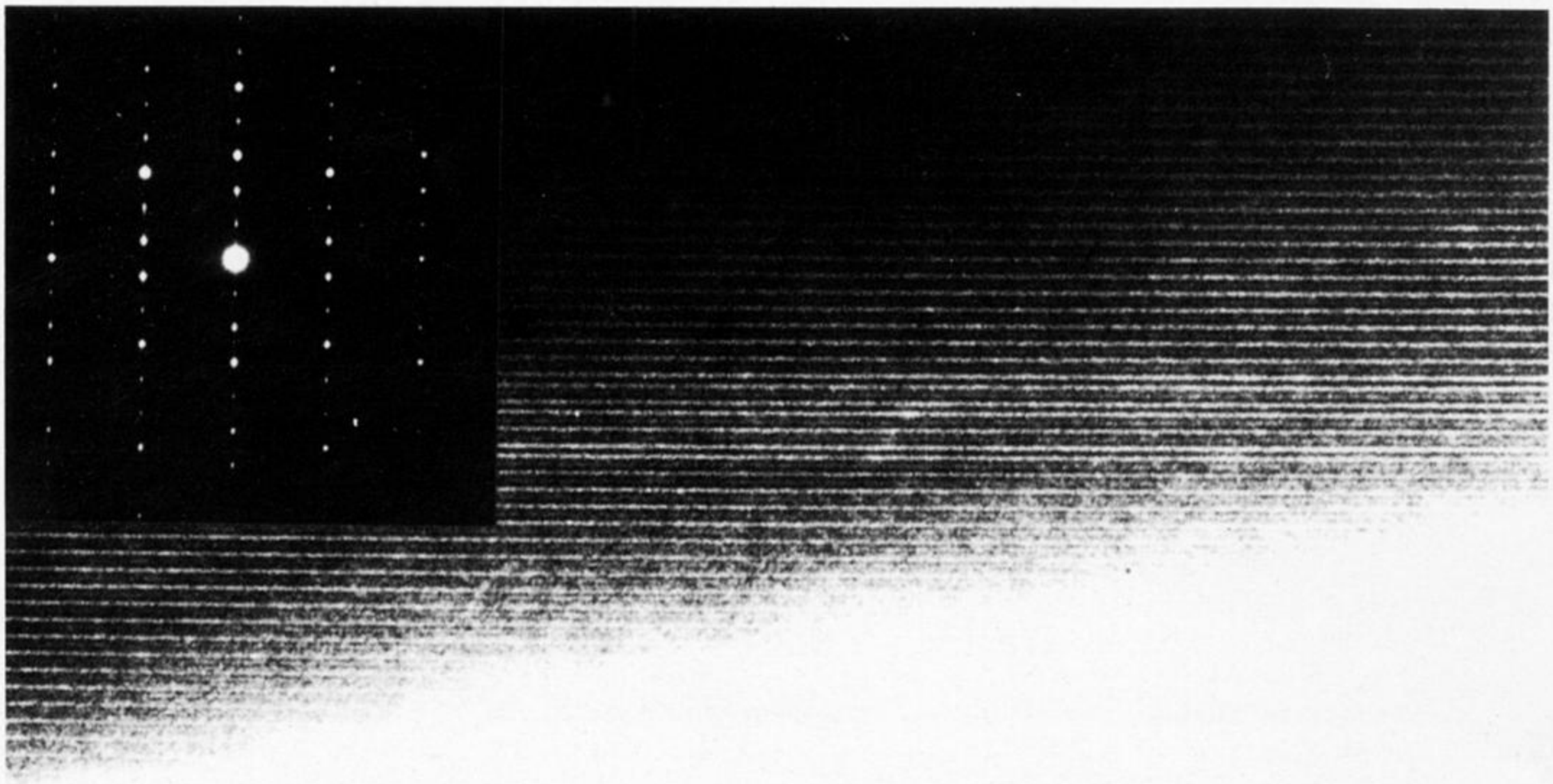

$La_3Ni_2O_7$ (1.66)

10 nm

(*a*)

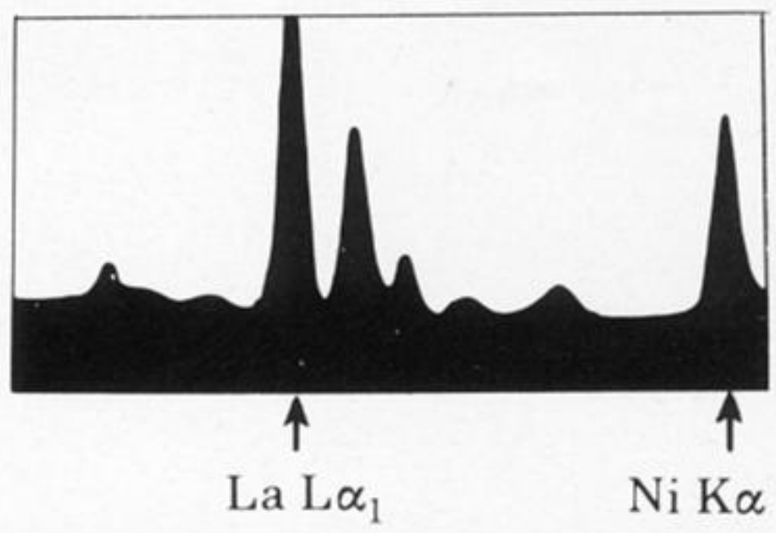

(*b*) $La_4Ni_3O_{10}$ (1.20)

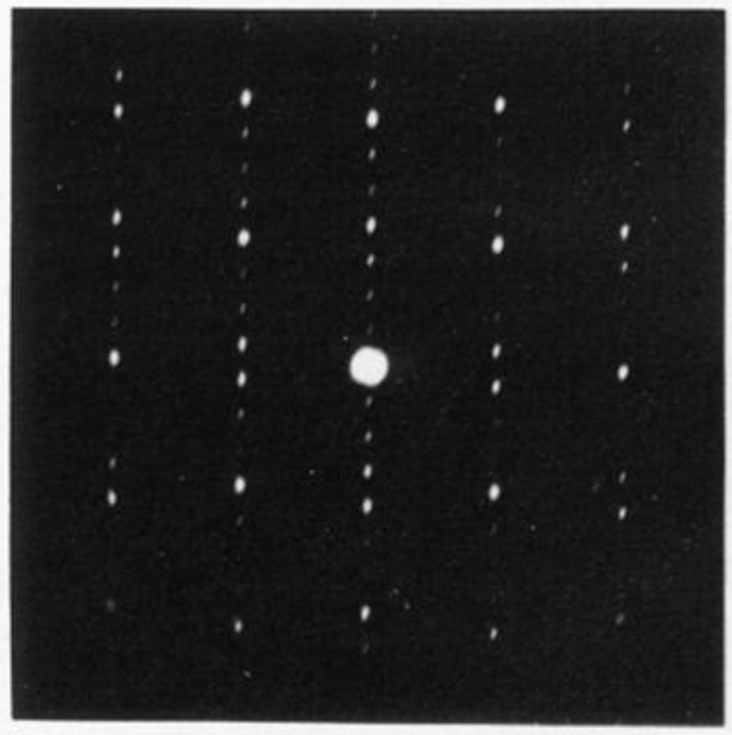

FIGURE 9. (*a*) Combined high-resolution lattice image, electron diffraction pattern and X-ray emission spectrum of a crystal of $La_3Ni_2O_7$. Defects in the structure are arrowed. (*b*) As for (*a*), but with a crystal of $La_4Ni_3O_{10}$.